



BRNO UNIVERSITY OF TECHNOLOGY
VYSOKÉ UČENÍ TECHNICKÉ V BRNĚ

FACULTY OF INFORMATION TECHNOLOGY
FAKULTA INFORMAČNÍCH TECHNOLOGIÍ

DEPARTMENT OF INTELLIGENT SYSTEMS
ÚSTAV INTELIGENTNÍCH SYSTÉMŮ

COUNTING PEOPLE USING A PIR SENSOR
POČÍTÁNÍ OSOB POMOCÍ PIR SENZORU

BACHELOR'S THESIS
BAKALÁŘSKÁ PRÁCE

AUTHOR **MARTIN BENEŠ**
AUTOR PRÁCE

SUPERVISOR **prof. Ing., Dipl.-Ing. MARTIN DRAHANSKÝ, Ph.D.**
VEDOUCÍ PRÁCE

BRNO 2018

Abstract

PIR (passive infrared) sensor are mainly used to detect a presence of a person and notifying a system to react appropriately. The aim of this thesis is to use the PIR sensors to recognize position of person, speed and direction of movement or count of people. To do so, thesis suggests a heat signal processing pipeline including wavelet transformation feature extraction, classifier and fuzzy logic system, collecting data from multiple sensors, processing them and merging them together into a result.

Abstrakt

PIR (pasivní infračervený) senzor se používá zejména pro detekci přítomnosti osoby a oznámení systému pro příslušnou reakci. Zaměřením této práce je užití PIR senzorů pro rozpoznávání pozice osoby, rychlosti a směru pohybu nebo počtu lidí ve snímaném prostoru. Za tímto účelem je navržen způsob zpracování jeho výstupního analogového signálu, počínající extrakcí příznaků pomocí vlnkové transformace, následnou klasifikací a generování výstupu na základě sběru dat z více senzorů pomocí speciálního systému, který ze vstupní matici fuzzy čísel generované klasifikátorem pro každý senzor generuje na výstup pozice přítomných osob.

Keywords

Sem budou zapsána jednotlivá klíčová slova v anglickém jazyce, oddělená čárkami.

Klíčová slova

Sem budou zapsána jednotlivá klíčová slova v českém (slovenském) jazyce, oddělená čárkami.

Reference

BENEŠ, Martin. *Counting People Using a PIR Sensor*. Brno, 2018. Bachelor's thesis. Brno University of Technology, Faculty of Information Technology. Supervisor prof. Ing., Dipl.-Ing. Martin Drahanský, Ph.D.

Counting People Using a PIR Sensor

Declaration

Prohlašuji, že jsem tuto bakalářskou práci vypracoval samostatně pod vedením pana X... Další informace mi poskytli... Uvedl jsem všechny literární prameny a publikace, ze kterých jsem čerpal.

.....
Martin Beneš
March 3, 2019

Acknowledgements

V této sekci je možno uvést poděkování vedoucímu práce a těm, kteří poskytli odbornou pomoc (externí zadavatel, konzultant, apod.).

Contents

1	Introduction	2
2	State of the art	3
2.1	Physics of radiation	3
2.2	Temperature homeostasis	5
2.3	Radiation perception	6
2.4	Pattern recognition	9
3	Design Description	11
3.1	Sensor module	11
3.2	Data processing pipeline	12
4	Data	17
5	Implementation	19
5.1	Module	19
5.2	Collector	21
5.3	Visualizer	21
6	Experiments	22
7	User Interface	23
8	Conclusion	24
	Bibliography	25
A	PIR signal recording	27

Chapter 1

Introduction

Our body as same as everything surrounding us emits some radiation. The dominant wavelengths belong to the infrared spectrum and our body senses it as a heat. If we pass its significance for living creatures and the fact that the presence of the right amount of infrared radiation is essential for all the life as we know it, there is also a lot of usage in the industry or generally – technology.

Infrared waves are used in various devices. From nightvision devices, astronomical telescopes to personal electronics (infraport, TV remote controller). This thesis focuses on the usage in PIR sensors – electronic devices that changes its output based on the amount of received infrared radiation.

The PIR sensors are used around us a lot even though we might not know it. We all know the waving of hands towards the sensor in a hallway so the light would turn on and we could tie our shoes, or the self-opening door in shopping malls or self-rotating door in banks. These mechanisms mostly use PIR sensors.



Figure 1.1: PIR sensor: automatic doorway. [5]

PIR sensors offer even more than stating a presence of person. It is possible to process sensor output signal to get more information about sensed space - a position of person, a number of people. Especially when more sensors are used.

The localization using PIR is still matter of intense research, a number of articles has been written on it. This thesis suggests multisensor attitude and a usage of fuzzy logic to merge sensor's outputs.

Chapter 2

State of the art

2.1 Physics of radiation

In the modelled system equations calculating with infrared radiation are being used – to understand them properly it is necessary to describe what is a radiation, where does it come from and how can we measure it.

As it was already mentioned in the chapter 1, every object whose temperature is higher than absolute zero emits an electromagnetic radiation.

$$T_{obj} > 0 \text{ K} \equiv -273.15^\circ\text{C} \quad (2.1)$$

It is caused by a charged subatomical particles (electrons, protons) that are undergoing an acceleration, emitting an energy in a form of photon – electromagnetic radiation.

Characteristics

The electromagnetic radiation have a number of measurable characteristics. The most significant ones are *frequency* f and *wavelength* λ . Due to the constant speed of the radiation v aka speed of light $c = v = 3 \cdot 10^8 \text{ m} \cdot \text{s}^{-1}$ not dependent on the frequency, they are proportional and mutually transferrable.

$$f = \frac{v}{\lambda} = \frac{c}{\lambda} = \frac{3 \cdot 10^8}{\lambda} \quad (2.2)$$

Electromagnetic waves are being divided into categories according to their usage by the wavelength λ . With increasing wavelength λ it is gamma, X-rays, ultraviolet (UV), visible light, infrared (IR) and radio waves. This is called electromagnetic spectrum and it is shown in the image 2.1.

Another measurable characteristic is an energy of the radiation Q, E or W . It is linearly dependend on its frequency f and can be computed using Planck constant $h = 6.63 \cdot 10^{-34} \text{ J} \cdot \text{s}$. [17]

$$W = h \cdot f \quad (2.3)$$

The power of the radiation Φ is called *radiant power* or rather *radiant flux*. As a regular power it is energy per time, since the radiation is four-dimentional, partial derivations must be used.

$$\Phi = \frac{\partial W}{\partial t} \quad (2.4)$$



Figure 2.1: Electromagnetic spectrum.

Name	Symbol	Unit	Definition
Radiant flux	Φ	W	Power transferred by a radiation.
Radiant exitance	M	$W \cdot m^{-2}$	Sent W per sender's surface.
Irradiance	E	$W \cdot m^{-2}$	Received W per receiver's surface.
Radiant intensity	I	$W \cdot sr^{-1}$	W per unit solid angle.
Radiance	L	$W \cdot sr^{-1} \cdot m^{-2}$	I per sender's area projected to a direction.

Table 2.1: Radiation characteristics. [15]

The radiant power per unit surface is a flux density. It is called either *radiant exitance* M when emitting or *irradiance* E when receiving.

$$M = \frac{\partial \Phi_{emitted}}{\partial S_{sender}} \quad (2.5a)$$

$$E = \frac{\partial \Phi_{received}}{\partial S_{receiver}} \quad (2.5b)$$

The Stefan-Boltzmann law defines irradiance of electromagnetic radiation as

$$I = \sigma \cdot T^4 \quad (2.6)$$

where $\sigma = 5.6704 \cdot 10^{-8} Wm^{-2}K^{-4}$ is the Stefan-Boltzmann constant and T is a thermodynamic temperature.

Power per unit solid angle I is called *radiant intensity*. With dividing by an area of the item projected from certain direction we get an amount of power emitted in that direction called *radiance* L .

$$I = \frac{\partial \Phi}{\partial \Omega} \quad (2.7a)$$

$$L = \frac{\partial I}{\partial S \cos(\theta)} \quad (2.7b)$$

Other characteristics of radiation can be seen in the table 2.1. [12] [15]

2.2 Temperature homeostasis

The animal bodies require physical and chemical conditions in order to work properly (or at all). One of the physical aspects is a temperature. There are generally three types of animals – *ectotherms*, *endotherms* and *mesotherms*.

Ectotherms do not regulate its body temperature and rely on an external source, endotherms keeps it constant independently on the environment, so called *homeothermy*¹. Mesotherm strategy is then something in between.

Endotherm groups are birds and mammals, the most significant ectotherm group are reptiles. They compensate it with basking in the sun. The thermal characteristics of these groups can be seen in the figure 2.2.



Figure 2.2: Thermal regulation graph.[10]

Human body temperature T_{HB} varies in $\langle 36^{\circ}C; 38^{\circ}C \rangle$, in the hyperthermia it can rise up to $40^{\circ}C$. The figure 2.3 shows the radiation wavelength composition. The peak wavelength (temperature $37^{\circ}C$ or 310.15 K) can be calculated with the Wien's displacement law.

$$\lambda_{max} = \frac{b}{T} = \frac{2.8977729 \cdot 10^{-3}}{310.15} = 9.3431 \mu m \quad (2.8)$$

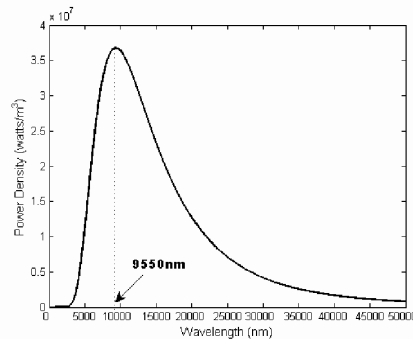


Figure 2.3: Human body radiation wavelength.[14]

¹Homeothermy is an aspect of homeostasis. It means keeping its inner body temperature within the preset limits.

2.3 Radiation perception

Radiation processed by organisms

This thesis describes a particular way how to use the infrared radiation. Very important beginning of such work is always studying existing applications. Unforgettable one is a nature – how evolution enabled various organisms to use it.

Many animals can process parts of electromagnetic spectrum. Eyes enables mammals, cephalopods and arthropods to sense a visible light, some insects can even see a part of UV. Additionally organisms including human often have thermoreceptors in their skin so they can get information about intensity of infrared radiation around them.

Visible light PIR sensor structure is obviously inspired by a human eye. Human eyes can process radiation $\lambda \in \langle 380 \text{ nm}; 760 \text{ nm} \rangle$ called visible light, one of the bands of an electromagnetic spectrum. Seeing means receiving a light from a light source reflected by the surface of an observed object to our retina. A biological system composed of light-sensitive cells *rods* and *cones* propagates the information through nerves to brain.

A ray coming to an eye is going through a converging lens, which changes its trajectory aiming to the retina, in the best case to the most sensitive place with a lot of the rods and cones called *Fovea centralis*. [24]



Figure 2.4: Structure of an eye. [3]

Heat The infrared rays surrounds us during our whole life, we sense it as heat. The heat receptors called *thermoreceptors* in our body are located on its surface (in the skin), but also in organs. The structure of a skin is shown in the figure 2.5.

There is a difference between sensing a visible light and an infrared radiation. Visible light comes mostly reflected from the surface, while the IR can originate only from the primary source – warm item.

Our skin contains two types of thermoreceptors: sensing cold, colder than a body temperature and hot, hotter than a body temperature. The skin structure is shown in the figure 2.5. This is already well described, on the other hand the evaluation center of these receptors in the brain and its mechanisms is not fully understood yet and a matter of current research. [13]

Some animals even use sensing the heat as a primary way how to survive. Several groups of snakes (pythons, rattlesnakes, boas and others) use it when hunting warm-blooded animals (mouses, rats, rabbits etc.). Blood-eating organisms (vampire bats, south-american heteroptera *Triatoma infestans*) have IR receptors to look for a vein under the skin.[6]

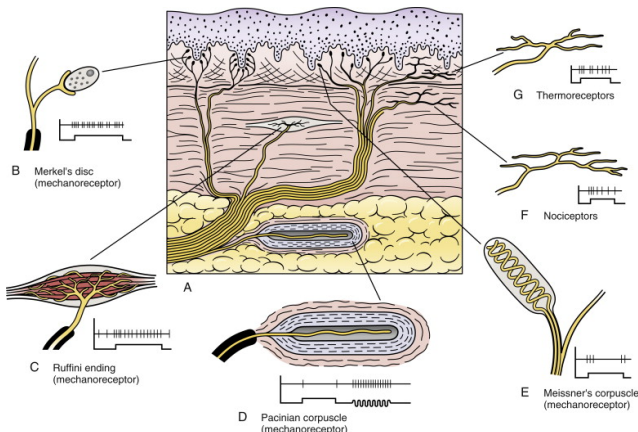


Figure 2.5: Structure of a skin. [8]

Discovery For the first time, the infrared electromagnetic waves were observed and named in 1800 by German-English astronomer sir Frederick Harschel. He dispersed light by a prism and found out that the temperature of the light is growing with wavelength, the red light had the highest one.

When he measured the temperature behind the red light, there was no visible light on the table but the thermometer was showing even higher temperature moving beyond the red spectrum. Harshel pronounced hypothesis that except the visible light there must be also invisible one which we can not see. [1]

A great coincidence is that he was an astronomer, he even discovered the planet Uranus, and it is his discovery, the IR waves, which now enables us to explore and understand the universe. [20]

Infrared radiation processed by machines

PIR (*passive infrared*) sensor is an electronic device that scans electromagnetic radiation at wavelength $\lambda \in \langle 700 \text{ nm}; 2.5 \text{ mm} \rangle$ aka frequency $f \in \langle 120 \text{ MHz}; 430 \text{ THz} \rangle$. [7]

Principles of PIR sensor There is a number of approaches how to construct such a sensor. The point is to convert the electromagnetic energy in electric voltage and send it away via wire to be processed by hardware or software.

First way how to do it is a *bolometer*. It uses the fact that resistance of a resistor is different when changing a temperature, as shown in the equation 2.6 for temperature difference ΔT and resistor with original resistance R_0 and new resistance R_t and with temperature coefficient α . So with using the same voltage it measures the electric current and with the Ohm law $R = \frac{U}{I}$ the sensor computes instantaneous resistance.

$$R_t = R_0(1 + \alpha\Delta T) \quad (2.9)$$

Figure 2.6: Relationship of resistance and temperature.

Another type is a *thermoelectric sensor* reacting to the different thermoelectric resistance of exposed wire and comparative wire.

The last is a *pyroelectric detector*. The principle is based on electrostatic polarization, changing during the temperature change. [16]

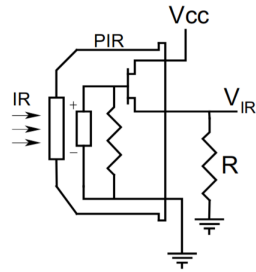


Figure 2.7: Single element pyroelectric detector.[7]

Sensing of the infrared radiation The structure of PIR sensor is inspired by structure of an eye described in subsection 2.3. An infrared ray incoming to the sensor first goes through *Fresnel lens* aiming it onto a pyroelectric sensor as you can see in the figure 2.8. Then the ray is transformed in an electric voltage.

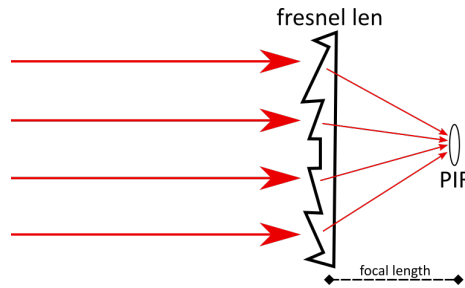


Figure 2.8: Fresnel lens.

Before the output the signal is being processed. For vast majority of application we are interested in people sensing emitting radiation characterized in the figure 2.3. Therefore the signal is amplified and filtered to well discriminate their presence and absence. An example is a scheme 5.1 of product *PIR STD* made by *B+B Sensors*.

Description of fresnel len of PIR STD.

2.4 Pattern recognition

The pattern recognition means processing of a signal and localizing of predefined objects. The form is dependent on the type of signal and the objects that we search. Generally we can say there are five parts of recognition pipeline.

Sensing

In the world of digital computers sensing means *sampling*, converting a continuous signal into discrete samples. It is present if the signal is being processed online.

Through different signal types various technologies for sensing are used – image, sound, temperature, pressure, weight, smell etc. The sensing procedure in the case of heat signal is described in the section 2.3.

There is a few things that we need to deal during sensing: noise, linearity, calibration, ageing.

Segmentation

The signal is splitted into segments by the time axis that are being processed separately. They can even overlap. Segmentation ensures fast processing saving memory and other resources.

Features extraction

Features are quantitative expression of the input signal, they replace the signal in the following phases. Its purpose is to reduce memory and computational complexity of the processing. Each segment of N samples is transformed to vector of K features, the point is to reduce dimensions, $K \ll N$, but preserve relevant characteristics. Choosing the right features is therefore key for the following classifier.

To have good results the features should be discriminative (distinguish between classes), invariant to the transformations (translation, rotation, scale, deformation etc.) and decorrelated - mutually independent.

Vast number of described ways how to create features exists – *Principal Component Analysis* (PCA), *Linear Discriminant Analysis* (LDA). They can be used generally, but there is also many special application-dependent features.

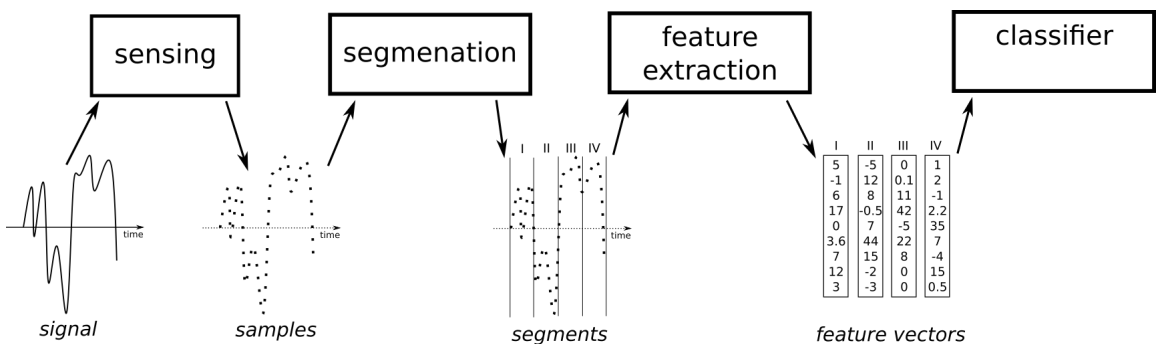


Figure 2.9: Components processing a signal before the classification itself.

Multiple thesis and articles were written on the topic of heat signal processing. For the feature extraction, [23] suggests *Wavelet Transformation*, [21] uses *chirplet*-based features, but also tests other feature-extraction methods: PCA, Expanded-Class LDA or fusion of PCA and LDA feature vectors, [11] calculates with the signal itself.

Classification

Before we will describe the classification phase, several terms must be defined:

- *Detection* is a classifying of presence of observed object or characteristic.
- *Identification* is an assigning the observed object to one of N classes.
- *Detection Error Tradeoff* is a relation of miss to false alarm probability of a classifier. The goal is minimizing both with finding the best settings of classifier parameters.

This thesis performs a detection of a presence of a person. In the case of positive detection identification of the situation is made – what was actually detected and whether it is a person or more people etc.

Finding the most suitable classifier for the task is fundamental, but consequent to the feature extraction method we use. At the end of the day, inputs of all the methods is a vector of features for each segment. There are linear and non-linear classifiers, separating the hyperdimensional space into segments. Then the segment is detected or identified if features vector geometrically lies in the right segment.

It is also possible to perform some kind of transformation before classification if the space is not separable linearly. But other attitudes are also possible like algorithm *K-nearest neighbors*.

An output of a classifier can be either a hard decision or some kind of soft score, which can be later processed by a postprocessor – used to merge data from more classifiers or something else. A classical linear classifier is used in *Linear Regression* or *Support Vector Machine* (SVM). Each neuron of recently very popular *Neural Networks* (NN) can also be represented with linear classifier.

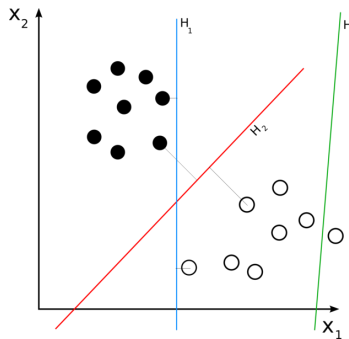


Figure 2.10: Linear classifier.[4]

Postprocessing

During postprocessing different information than pattern are used, procedure is connected to the concrete task. This parts often includes hard decision, if the classifier's output is a soft score – prices are taken into consideration, the simplest way is using treshold.

Chapter 3

Design Description

The design of the whole project is separated in two modules - sensor module and visualization program. Sensor module senses the observed space and does the signal processing of outputs of connected PIR sensors. The data are then collected and the fusion is made over them.

Results might be displayed in the visualization program. The data are being sent over network. In the implementation, LAN is used, but it could be possible to use the Internet and send the data to the remote visualizer.

3.1 Sensor module

Sensor module is a board with fixed sensors on it and a microcontroller performing the classification process described in subsection 3.2.

The sensors signal is at the end fused together and the results are classified objects with coordinates in polar coordinate system relative to the module position. These coordinates are sent to the client.

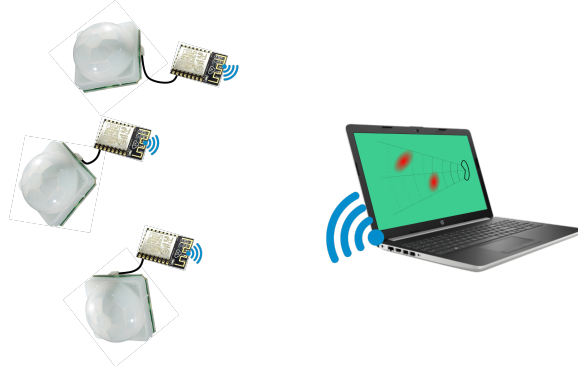


Figure 3.1: Geometry for three PIR sensors.

The interior angle of module Ω is a parameter of the module construction. Using this parameter orientation λ and position $p_X = (d_X, \varphi_X)$ ¹ of sensors can be expressed.

¹Position uses polar coordinates with the origin in the central sensor.

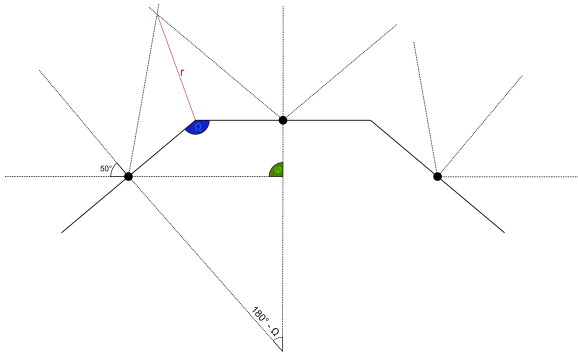


Figure 3.2: Geometry for three PIR sensors.

Parameter r is length of module edges with sensor in the center. Sensor PIR-STD by B+B Sensors has $250 \times 250 \times 200$ mm; therefore $r > 250$ mm.

$$\lambda_C = 0 \quad (3.1a)$$

$$\lambda_L = -\lambda_R = 180 - \Omega \quad (3.1b)$$

$$\varphi_C = 0 \quad (3.2a)$$

$$\varphi_L = -\varphi_R = 90 + \frac{180 - \Omega}{2} \quad (3.2b)$$

$$d_C = 0 \quad (3.3a)$$

$$d_L = d_R = \frac{r}{2}(r - 4\cos(\Omega)) \quad (3.3b)$$

3.2 Data processing pipeline

The data path in the design is slightly inspired by classification phases except there is fuzzification used here. It enables to create a fusion logic over vague facts without need to evaluate them first.

Sensing Here we should think how to place sensor(s) in order to get the best results. Interesting solution is suggested in [19]. Three PIR sensors are placed on solid board, as shown in the figure 3.2.

This brings a great advantage – not only it enables using of more sensors at one time, but also it reduces the issue with positioning the sensors, since it is given by the board construction.

The key here is to find the best value for Ω to minimize r , but maximize φ . Low r means more reliable results. High φ increases measurable range. Unfortunately these parameters are inversely proportional, a compromise needs to be done.

Now let's express both observed parameters with Ω . A sensor has 250 mm to 250 mm, o is a size of empty space on the sides of sensor, equation substituted $L = (12.5 + o)$.

$$\varphi = 230 + \Omega \quad (3.4a)$$

$$r = \frac{\sin((\frac{\Omega}{2}))L}{\tg(\frac{\Omega}{2} - 40)} - \cos((\frac{\Omega}{2}))L \quad (3.4b)$$

Segmentation

The size of segments has a great influence on processing speed. And since the result should run in the real time, it is quite important.

Features extractions

Choosing good features is inevitable part of desing and the following classifier is strictly dependent on the form of features, since it is its input. Feature extraction and fuzzification is implemented in the program *collector*.

The input is a vector of N samples and the process transforms them into the vector of F features on the output.

$$\Psi_s(x) = \begin{cases} -1 & x \in (0; \frac{s}{2}) \\ 1 & x \in (\frac{s}{2}; s) \\ 0 & \text{otherwise} \end{cases} \quad (3.5)$$

Figure 3.3: Haar Wavelet.

$$\Psi(x) = e^{-\frac{x^2}{2}} \cos(5x) \quad (3.6)$$

Figure 3.4: Morlet Wavelet.

$$\Psi(x) = \frac{2^{\frac{5}{4}}}{\sqrt{3}} (1 + e^{2\pi x^2}) e^{-\pi x^2} \quad (3.7)$$

Figure 3.5: Mexican Hat Wavelet.

Wavelet transformation for feature extraction

Fuzzification and classification

The classifier fuzzifies received a F-sized feature vector representing a segment of samples sensed by a sensor into a 2D fuzzy values array. These values express fuzzy membership value of presence of a person.

Representation of the space in front of a sensor is inspired by cellular automata - carved into segments. These segments are given by azimuth (phase) with a center in the sensor and by the distance zone - deltas in polar coordinates.

Even though the space because of the construction of sensor has a shape of circular sector, it can be easily represented by classical 2D matrix, as it is shown in the figure 3.6.

Fuzzification. Consider action characteristics (speed, direction, multiple people).

The output of fuzzification is a 2D matrix of space segments containing fuzzy value expressing presence of person.

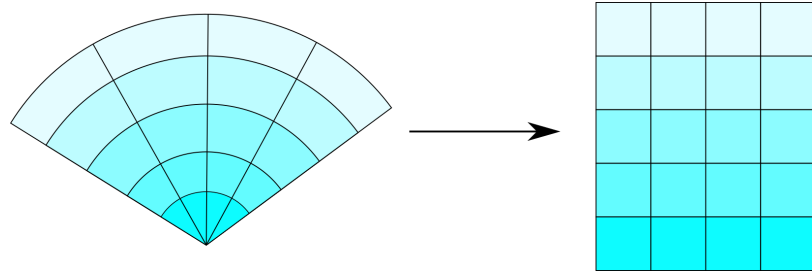


Figure 3.6: Representation of circular sector.

Using more sensors brings advantages: the measuring might be more precise since the person presence classified by two independent sensors is not only more probable but the computed position can get more accurate than when using only one sensor. The disadvantage is higher price and need to know the mutual orientation and position of the sensors.

If more sensors are used it is necessary to merge their space segments matrixes in one, as shown in the figure 3.7. To do so, a fuzzy logic mechanism *Takagi-Sugeno rules* can be used as described in [22]. The form of rules is [IF antecedent THEN succendent] as shown in the table 3.1. During the calculation all the antecedentes are evaluated and the most relevant leads to application of corresponding succendent to the output.

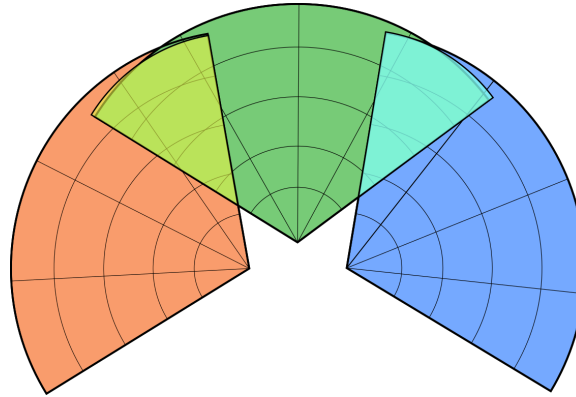


Figure 3.7: Fusion of detection areas.

Rule	Antecedent	Succendent
R_1	X_1 is A_{11} and ... and X_n is A_{1n}	$Y = b_{10} + b_{11}X_1 + \dots + b_{1n}X_n$
R_2	X_1 is A_{21} and ... and X_n is A_{2n}	$Y = b_{20} + b_{21}X_1 + \dots + b_{2n}X_n$
...		
R_m	X_1 is A_{m1} and ... and X_n is A_{mn}	$Y = b_{m0} + b_{m1}X_1 + \dots + b_{mn}X_n$

Table 3.1: Takagi-Sugeno rules. X is input, A is a matrix of fuzzy numbers, b is a matrix of fuzzy coefficients. [22]

The designed fusion fuzzy system is to be seen in the table 3.2. To be able to merge the space segments, overlap must be known and then vector X is created, containing pairs of values from each vector ($X[i]_L$ and $X[i]_R$). Each of these pairs is input to the fusion algorithm, which merges it to one fuzzy number result.

C_L and C_R are 2D matrixes of coefficients with indexing $[i, j]$, where $i, j \in \{0, L, M, H\}$. The fuzzy sets LOW, MEDIUM and HIGH of X composes a basic evaluative trichotomy extended for unknown state OUT. The optimal values of coefficients and the fuzzy sets parameters have to be found experimentally.

Rule	X_L	X_R	\mathbf{Y}	
R_1	OUT	OUT	$C_L[0, 0]$	$+ C_R[0, 0]$
R_2	OUT	LOW	$C_L[0, L]$	$+ C_R[L, 0]X_R$
R_3	OUT	MEDIUM	$C_L[0, M]$	$+ C_R[M, 0]X_R$
R_4	OUT	HIGH	$C_L[0, H]$	$+ C_R[H, 0]X_R$
R_5	LOW	OUT	$C_L[L, 0]X_L$	$+ C_R[0, L]$
R_6	LOW	LOW	$C_L[L, L]X_L$	$+ C_R[L, L]X_R$
R_7	LOW	MEDIUM	$C_L[L, M]X_L$	$+ C_R[M, L]X_R$
R_8	LOW	HIGH	$C_L[L, H]X_L$	$+ C_R[H, L]X_R$
R_9	MEDIUM	OUT	$C_L[M, 0]X_L$	$+ C_R[0, M]$
R_{10}	MEDIUM	LOW	$C_L[M, L]X_L$	$+ C_R[L, M]X_R$
R_{11}	MEDIUM	MEDIUM	$C_L[M, M]X_L$	$+ C_R[M, M]X_R$
R_{12}	MEDIUM	HIGH	$C_L[M, H]X_L$	$+ C_R[H, M]X_R$
R_{13}	HIGH	OUT	$C_L[H, 0]X_L$	$+ C_R[0, H]$
R_{14}	HIGH	LOW	$C_L[H, L]X_L$	$+ C_R[L, H]X_R$
R_{15}	HIGH	MEDIUM	$C_L[H, M]X_L$	$+ C_R[M, H]X_R$
R_{16}	HIGH	HIGH	$C_L[H, H]X_L$	$+ C_R[H, H]X_R$

Table 3.2: Design fuzzy system to fuseTakagi-Sugeno rules. X is input, A is a matrix of fuzzy numbers, b is a matrix of fuzzy coefficients. [22]

For three sectors as in the figure 3.7 the situation is analogous. The table also depends on whether the areas of the side sensors overlap or not. Or they can be merged successively.

Defuzzification

To get the results in a form of coordinate(s) of classified objects a cluster analysis is done. It calculates a clusters of high membership values, for optimization α -cut on a certain level or thresholded matrix can be used. Algorithm PAM (Partitioning Around Medoids is used), similar to k-means, where item called medoid is used to represent the cluster instead of mean.

$$PAM(k, data) = argmin \left(\sum_{i=1}^k \sum_{j=1}^k ||data_i - data_j|| \right) \quad (3.8)$$

```

1 def PAM(k, data):
2     # pick medoids
3     medoids = [] .generate(k, data.random())

```

```

4 # compute dissimilarity matrix
5 dm = DissimilarityMatrix(data,calculateDistance)
6 # create clusters
7 changed = True
8 while changed:
9     changed = False
10    clusters = []
11    for medoid_idx,medoid in medoids.enum():
12        cluster = []
13        for d in data:
14            # add to cluster with closest distance to its medoid
15            if dm[d,medoid] == dm[d,medoids].min():
16                cluster.append(d)
17        # set new center (SWAP phase)
18        cluster.append(medoid)
19        if medoid is not cluster.center():
20            medoids[medoid_idx] = cluster.center()
21            changed = True
22        clusters.append(cluster)
23 return clusters

```

```

1 function elbow(data):
2 # try all k
3 best = inf
4 for k in <1,K_MAX>:
5     clusters = PAM(data, k)
6     # take minimal
7     if WCSS(clusters) < best:
8         best = clusters
9 return best

```

To estimate the k , elbow method can be used: calculating k-means for different k values and taking the one with minimal within-cluster sum of square (WCSS).[9] [18]

$$WCSS = \sum_{i=1}^k \sum_{x \in S_i} \|x - \mu_i\|^2 \quad (3.9)$$

Very important is computing a distance of two segments. Since the original circular sector segmentation is not homogenous, the distances varies with each distance. It can be calculated though using cosine law. $P = (d, \alpha)$ is a segment given by polar coordinates, d is distance and α is azimuth.

$$|P_1P_2| = \sqrt{(d_1)^2 + (d_2)^2 - 2d_1d_2(\alpha_1 - \alpha_2)} \quad (3.10)$$

Chapter 4

Data

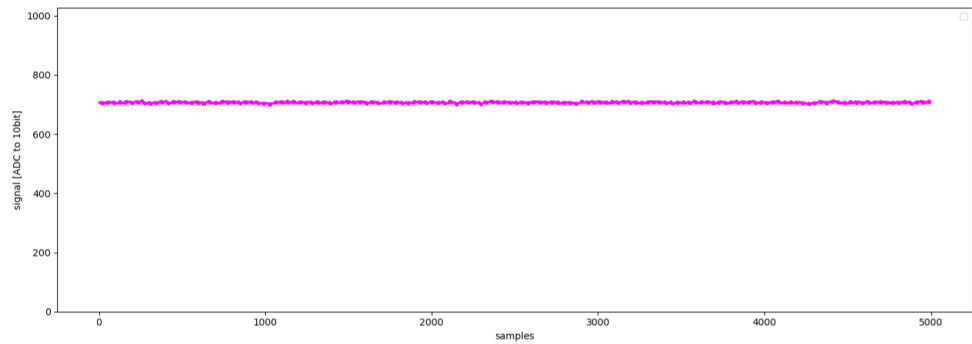


Figure 4.1: Signal of zero movement.

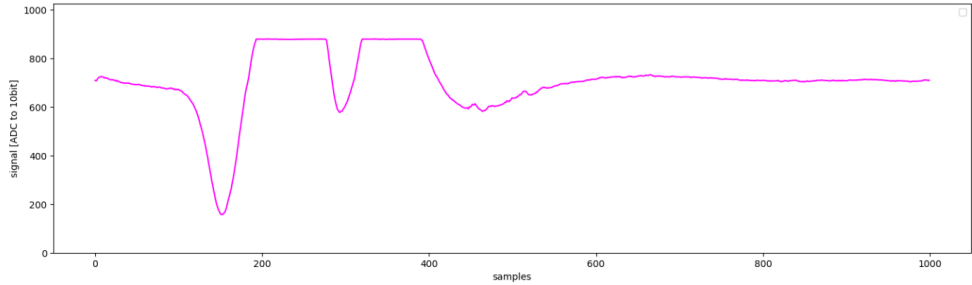


Figure 4.2: Signal of person walking around.

A output of a sensor as you can see in the figures 4.1 and 4.2 is very discriminative – with a bare eye a movement from no movement is distinguishable. A detection of presence used in light sensors can be implemented with thresholding, this attitude is not very suitable for classification of anything else except the presence itself.

In a calm state the sensor sends a constant signal¹. Movement in the sensed area causes abrupt changes of output. When the object either leaves the area, or stays completely calm,

¹Constant signal in the terms of electricity, slightly polluted with a background noise etc.

the signal changes are getting slower and after a little while the output voltage gets in the calm state again.

Therefore, the nature of the signal does not seem to need a complicated method to perform a classification on it. *Fourier transformation* and *wavelet transformation* were considered for feature extraction. The abrupt changes in the signal could be problem for FT, because it can not represent it efficiently[23], but unlike sinusoids, the wavelets exist for a finite duration and they are suitable for representing abrupt changes.

The wavelet transformation is defined as a function $F(s,k)$. Parameters s,k are scale and shift, changing them in predefined unit and interval creates a matrix, as you can see in the figure 4.4.

$$F(s, k) = \sum_{n=1}^N x[n]\Psi_{(s,k)}^*[n] \quad (4.1)$$

Firstly The data were offline analysed using *Matlab*, which has implemented wavelet transformation. The Matlab is not used because it is proprietary software and the program would be dependent on it. During the analysis it was found, that the data are very well separable using continuous wavelet transformation.

```
1 data = csvread('walk02.csv');
2 wscalogram('image', cwt(data));
```

Figure 4.3: Matlab code performing cwt.

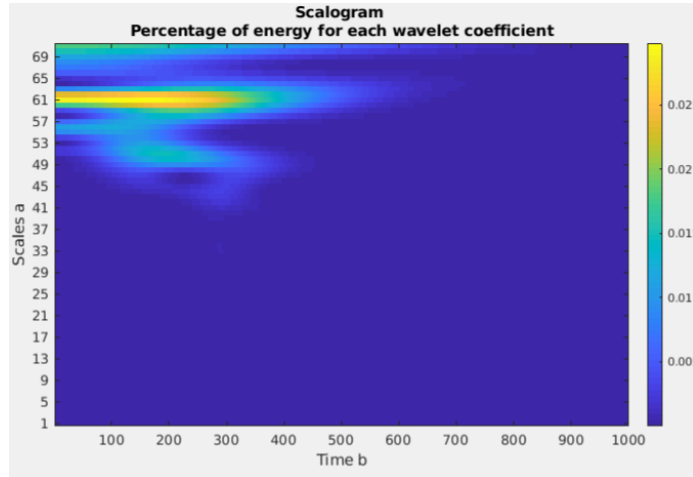


Figure 4.4: Matlab *cwt()* output of *walk03.csv*.

Origin of data, description, training.

The lab results are shown in the appendix A.

Chapter 5

Implementation

5.1 Module

Nowadays most of the PIR sensors sold have only a binary output. When signal reaches a set threshold output is set to logic „1“ for a unit of time. This mechanism is suitable for a light sensor or door sensor, completely useless for the needs of this project though.

The only found sensor that offers an analog output was *PIR STD* by *B+B Sensors*. *Add documentation to appendix.*

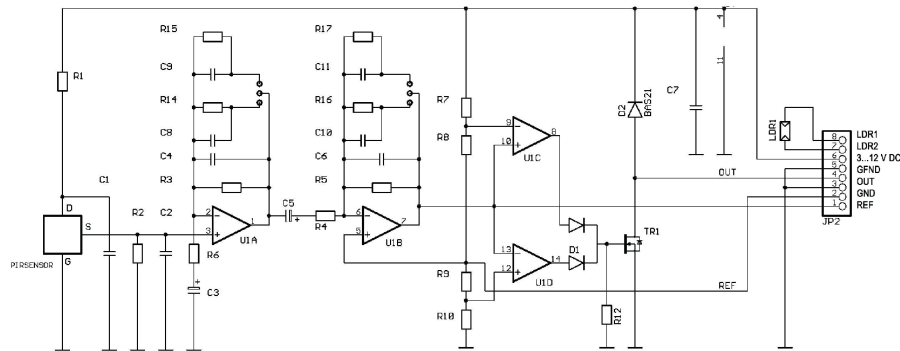


Figure 5.1: Scheme of PIR STD.

The *PIR STD* scheme shown in the figure 5.1 processes the signal in three stages going from left to right. The first two processes the signal to analog output. The third generates binary output from analog.

I. stage The first one starts at S of the PIR sensor, following with noise filter consisting of the amplifier $U1A$ and the feedback components $R3$, $C4$, $C8$, $R14$, $C9$, $R14$. There is also highpass filter done by $R6$ and $C3$. The output of this stage is a signal with frequency between f_{L1} and f_{H1} amplified A_{U1A} times.

$$f_{H1} = \frac{1}{2\pi R_{3,14} C_{4,8}} \quad (5.1a)$$

$$f'_{H1} = \frac{1}{2\pi R_{3,15} C_{4,9}} \quad (5.1b)$$

The choice of resistor $R_{3,14}/R_{3,15}$ and capacitor $C_{4,8}/C_{4,9}$ is done by connected switch. The value of resistance and capacitance of the components can be counted with formula for parallel connection.

$$R_{A,B}^p = \frac{1}{R_A} + \frac{1}{R_B} \quad (5.2)$$

$$C_{A,B}^p = C_A + C_B \quad (5.3)$$

The same for the resistors $R_{5,16}$ and $R_{5,17}$ and capacitors $C_{6,10}$ and $C_{6,11}$.

$$f_{L1} = \frac{1}{2\pi R_6 C_3} \quad (5.4)$$

$$A_{U1A} = 1 + \frac{R_{3,14}}{R_2} \quad (5.5a)$$

$$A_{U1B} = 1 + \frac{R_{3,15}}{R_2} \quad (5.5b)$$

II. stage The second processing stage focuses on amplification. It also includes lowpass filtering done by C_5 and R_4 and highpass filter performed by the feedback of amplifier $U1B$. The greater amplification is also made by the divider bridge (R_8, R_9, R_{10}, R_{11}) connected to the positive input. The output of frequency between $\max(f_{L1}, f_{L2})$ and $\min(f_{H1}, f_{H2})$ amplified $A_{U1A} \cdot A_{U1B}$ times is an analog output connected to the pin 1.

$$f_{H2} = \frac{1}{2\pi R_5 C_6} \quad (5.6)$$

$$f_{L2} = \frac{1}{2\pi R_4 C_5} \quad (5.7)$$

$$A_{U1B} = -\frac{R_5}{R_4} \quad (5.8)$$

III. stage The third phase performs top-bottom thresholding generating binary output used in simple industrial application. It is not used in the project.[2]

Programming of module

The module is programmed to read signal in sampling frequency and send the data to server.

The usable sampling frequency can be estimated: the fresnel lens of *PIR STD* splits the area into 10° circular sectors. Object moving around the sensor in the distance 0.5 m with speed $15\text{ km.h}^{-1} = 4.1667\text{ m.s}^{-1}$ (very fast run) passes the central circular sector in

$$t = \frac{s}{v} = \frac{0.5 * \text{tg}(10^\circ)}{4.1667} = 0.02116\text{ s} \quad (5.9)$$

This means the frequency of the movement through the circular sectors is

$$f = \frac{1}{t} = \frac{1}{0.02116} = 47.259\text{ Hz} \quad (5.10)$$

According to Shannon theorem, the sampling frequency must be at least twice as big as the maximal frequency in the signal, which leads to

$$Fs \geq 2 * 47.259 = 94.518 \quad (5.11)$$

Rounding up gives us minimal sampling frequency 100 Hz , or sampling period 10 ms . resulting with $2B$ sample in throughput N

$$N = Fs * |\text{sample}| * 8 \frac{\text{bit}}{\text{byte}} = 100 * 2 * 8 = 1.6 \text{ kbps} \quad (5.12)$$

5.2 Collector

Collector is a program, as the name says, that collects data from sensors and implements the whole described algorithm. Classified objects are then sent to a *visualizer*.

Communication

The communication of the sensor module and the client app is designed as a client-server. The results from the classification performed by server are sent to the client which shows it to user.

As the technology for the channel a LAN multicast stream is used at $224.0.0.128:12345$. The main advantage in comparison to unicast is a support of multiple clients.

5.3 Visualizer

Client app called *Visualizer* is written in *Python3* and graphical library *Tkinter*. This choice was made with portability of the program taken into consideration. The design of user interface is described in chapter 7.

Chapter 6

Experiments

Unit tests were created to verify the program components. It uses *Boost.Test*, framework for creating unit tests which is part of *C++ Boost* library set. The testing program placed in folder *collector/tests/* is linked with *collector* transformed in static library.

Metodika a vysledky. Muze zahrnovat i matematicke dukazu, postupy...

Interpretace vysledku a moznosti nasazeni v praxi.

HW narocnost – CPU, pamet, chovani pri paralelizaci apod.

Chapter 7

User Interface

Description of visualizer

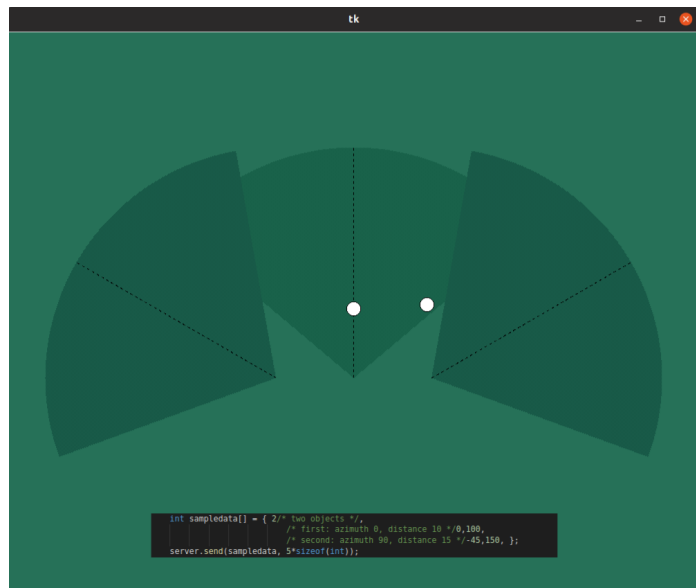


Figure 7.1: Visualizer prototype with sample data. *Will be replaced.*

Chapter 8

Conclusion

Shrnuti zameru prace. Zhodnoceni splneni (i formálnich bodů).

Zhodnocení z pohledu dalsího vývoje. Co se nestihlo (a dalo by se jít).

Bez odkazu do textu / literatury. Zadné nové poznatky, čísla a grafy.

Pekný postřeh k práci (co jsem se naučil).

Vyhled do budoucna, rozdelení na části.

20 stranek SEP, 40 bakalárka.

Bibliography

- [1] Caltech: *Herschel Discovers Infrared Light*. IPAC Caltech. [Online; visited 14.12.2018].
Retrieved from: http://coolcosmos.ipac.caltech.edu/cosmic_classroom/classroom_activities/herschel_bio.html
- [2] Colliard-Piraud, S.: *Signal conditioning for pyroelectric passive infrared (PIR) sensors*. AllAboutCircuits. July 2016. [Online; visited 18.2.2019].
Retrieved from: <https://www.allaboutcircuits.com/industry-articles/signal-conditioning-for-pyroelectric-passive-infrared-sensors/>
- [3] Cox, E.: *Optics of the Human Eye*. carolina.com. December 2016. [Online; visited 23.12.2018].
Retrieved from: <https://www.carolina.com/teacher-resources/Interactive/optics-of-the-human-eye/tr39501.tr>
- [4] Cyc: *SVM Separating Hyperplanes*. Wikipedia. February 2008. [Online; visited 23.12.2018].
Retrieved from:
https://commons.wikimedia.org/wiki/File:Svm_separating_hyperplanes.png
- [5] Duncan, R.: *Automatic doorway*. PublicDomainFiles. December 2018. [Online; visited 14.12.2018].
Retrieved from:
http://www.publicdomainfiles.com/show_file.php?id=13392932418863
- [6] E.O. Gracheva, N. I.: *Molecular basis of infrared detection by snakes*. *Nature*. 2010. doi:10.3410/f.2579956.2234055.
- [7] Ess, D. V.: *Pyroelectric Infrared Motion Detector*. [Online; visited 15.12.2018].
Retrieved from: <https://cdn-learn.adafruit.com/assets/assets/000/010/138/original/an2105.pdf>
- [8] Gregory D. Cramer, S. A. D.: *Clinical Anatomy of the Spine, Spinal Cord, and Ans*. Elsevier. 2014. ISBN 978-0-323-07954-9.
- [9] Hana Řezanková, V. S., Dušan Húsek: *Shluková analýza dat*. Professional Publishing. 2009. ISBN 978-80-86946-87-8.
- [10] Hawer, J.: *Thermal regulation graph*. Wikipedia. May 2018. [Online; visited 15.12.2018].
Retrieved from:
https://commons.wikimedia.org/wiki/File:Thermal_Regulation_Graph.svg

- [11] Hyun Hee Kim, S. L., Kyoung Nam Ha: *Resident Location-Recognition Algorithm Using a Bayesian Classifier in the PIR Sensor-Based Indoor Location-Aware System*. 2009. doi:10.1109/tsmcc.2008.2008099. [Online; visited 22.12.2018].
- [12] Quantities and units – Part 7: Light. Standard. International Organization for Standardization. Geneva, CH. November 2008.
- [13] J. Brendan Ritchie, P. C.: *The bodily senses*. Oxford University Press. 2015. ISBN 0-19-960047-3.
- [14] Jian-Shuen Fang, D. J. B., Qi Hao: *Path-dependent human identification using a pyroelectric infrared sensor and Fresnel lens arrays*. Optics express. February 2006. doi:10.1364/OPEX.14.000609. [Online; visited 23.12.2018].
Retrieved from: https://www.researchgate.net/figure/Black-body-radiation-curve-of-human-body-at-37-o-C_fig1_26273296
- [15] Kreidle, M.: *Měření teploty - senzory a měřící obvody*. BEN - technická literatura. 2005. ISBN 80-7300-145-4.
- [16] Lysenko, V.: *Detektory pro bezdotykové měření teplot*. BEN - technická literatura. 2005. ISBN 80-7300-180-2.
- [17] NASA: *The Electromagnetic Spectrum*. NASA webpage. March 2013. [Online; visited 14.12.2018].
Retrieved from:
<https://imagine.gsfc.nasa.gov/science/toolbox/emspectrum2.html>
- [18] Půlpán, Z.: *Odhad informace z dat vagní povahy*. Academia. 2012. ISBN 978-80-200-2076-5.
- [19] Raes, G.-W.: *Infrared Body Sensing*. Logos Foundation. October 2007. [Online; visited 5.1.2018].
Retrieved from: https://www.logosfoundation.org/ii/infrared_sensing.html
- [20] Smith, S.: *What is Infrared Radiation?* YouTube. [Online; visited 14.12.2018].
Retrieved from: <https://www.youtube.com/watch?v=KwvXcUe100Q>
- [21] Tarun Choubisa, S. B. M., Mohan Kashyap: *Comparing chirplet based classification with alternate feature-extraction approaches for outdoor intrusion detection using a pir sensor platform*. 2011. doi:10.1109/CISP.2017.8125869. [Online; visited 22.12.2018].
- [22] Vilém Novák, A. D., Irina Perfilieva: *Insight Into Fuzzy Modelling*. Wiley. 2016. ISBN 9781119193180.
- [23] Wang, L.: *Human infrared signal recognition using single PIR detector*. 2017. doi:10.1109/ICACCI.2017.8125869. [Online; visited 22.12.2018].
- [24] WikiLectures: *Light, eye and vision*. WikiLectures. [Online; visited 14.12.2018].
Retrieved from: https://www.wikilectures.eu/w/LIGHT,_EYE_AND_VISION

Appendix A

PIR signal recording

The movements that data shows were prepared in several directions and the type of movement can be read from the figure captions.

The trajectories are concentrated circles with sensor in center and radius values 3 m, 6 m, 9 m and 12 m. The direction is either left-to-right (LR) or right-to-left (RL). ¹ The movement was recorded multiple times.

Other cases are recorded as well: person walking towards (*C_BF*) or walking away (*C_FB*) from the sensor and no movement (*E*).

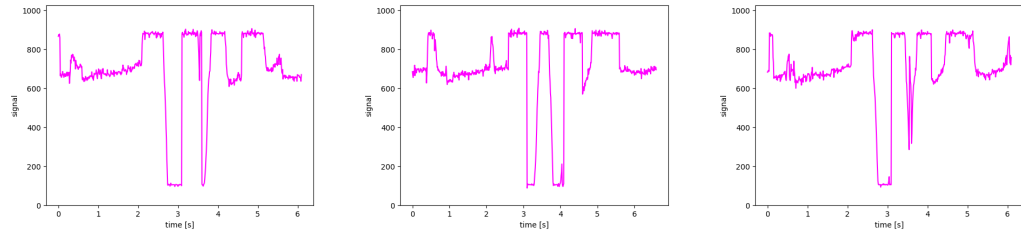


Figure A.1: 3m_LR.

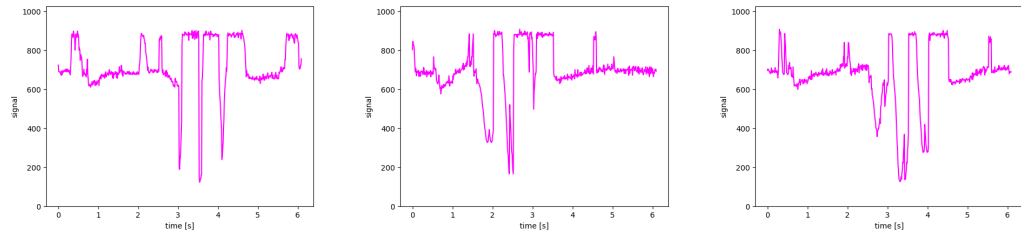


Figure A.2: 3m_RL.

¹For example 6m_RL is movement 6 m from sensor right-to-left.

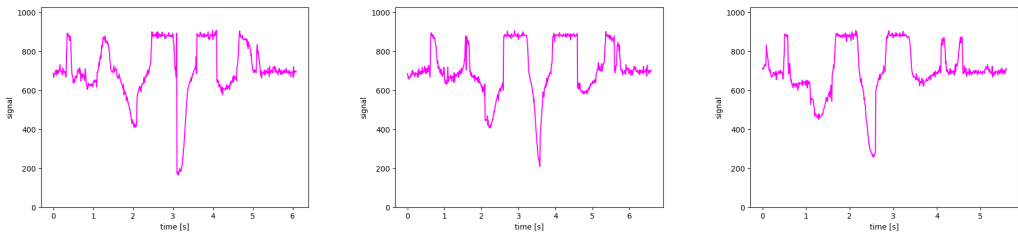


Figure A.3: 6m_LR.

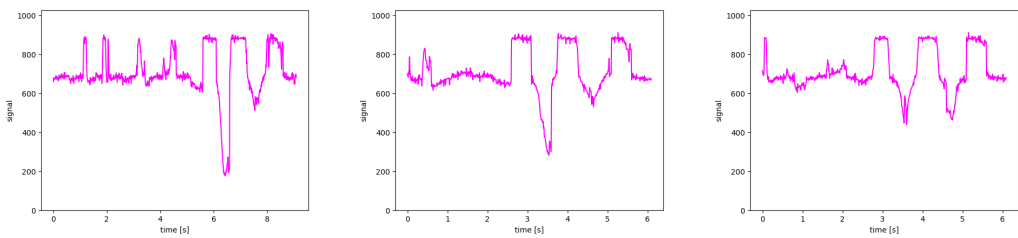


Figure A.4: 6m_RL.

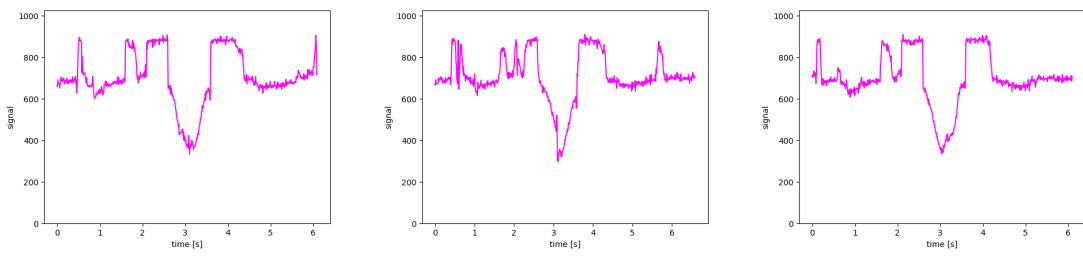


Figure A.5: 9m_LR.

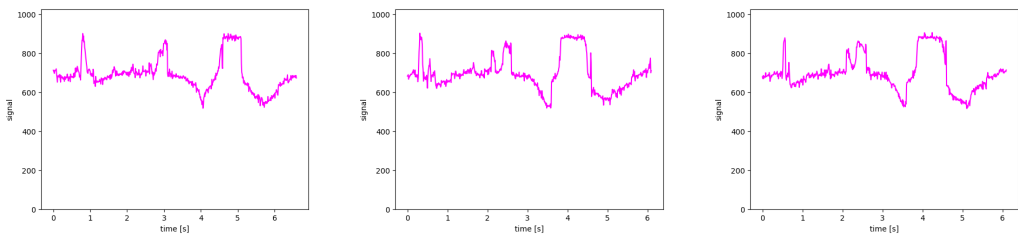


Figure A.6: 9m_RL.

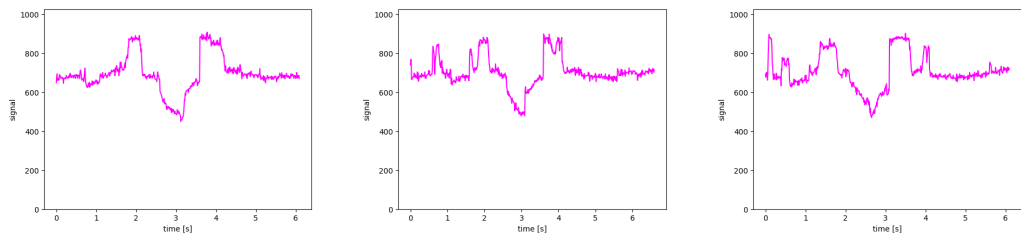


Figure A.7: 12m_LR.

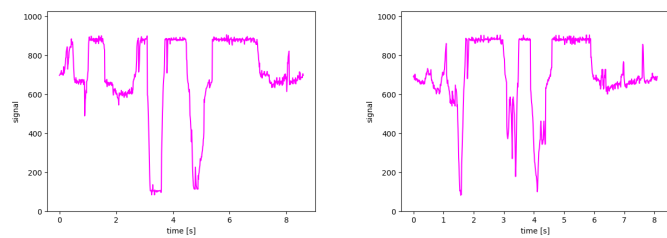


Figure A.8: C_BF.

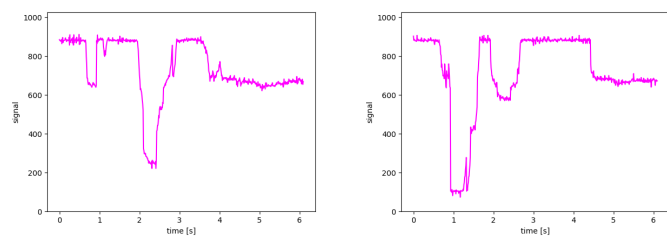


Figure A.9: C_FB.

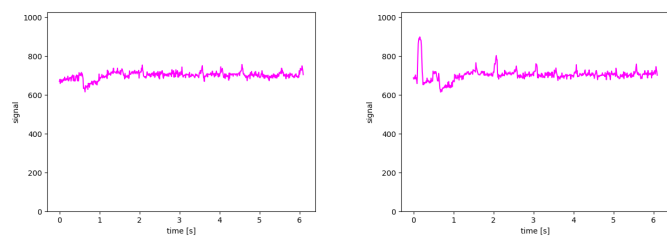


Figure A.10: E.